Available online at www.sciencedirect.com

ScienceDirect

journal homepage: www.elsevier.com/locate/he

Raman *in situ* characterization of the species present in Co/CeO_2 and Co/ZrO_2 catalysts during the COPrOx reaction

*Leticia E. Gómez, John F. Múnera, Brenda M. Sollier, Eduardo E. Miró, Alicia V. Boix**

Instituto de Investigaciones en Catálisis y Petroquímica — INCAPE (FIQ, UNL-CONICET), Santiago del Estero 2829, 3000 Santa Fe, Argentina

ARTICLE INFO

Article history:
Received 11 September 2015
Received in revised form
27 November 2015
Accepted 19 January 2016
Available online 15 February 2016

Keywords:
COPrOx
Cobalt
In situ Raman

ABSTRACT

The *in situ* Raman spectroscopy constitutes a powerful procedure to characterize catalytic surfaces under reaction conditions. In this work, we studied the species present in Co/CeO_2 and Co/ZrO_2 catalysts during the COPrOx reaction carried out between room temperature and 500 °C. For both catalysts, TPR and Raman results suggest that a redox mechanism proceeds in which the reduction step with either hydrogen or CO is the rate-limiting step. The CeO_2 support is better than the ZrO_2 one because the former accelerates the surface exchange between reduced and oxidized species due to the high mobility of surface lattice oxygen and the presence of oxygen vacancies. The $Ce^{4+} + Co^{2+} \leftrightarrow Ce^{3+} + Co^{3+}$ process acts as a buffer effect by which Co^{3+}, which is the active species in this reaction, is always present even in a reducing atmosphere, as shown by *in situ* Raman characterization.

Introduction

The global demand for energy has been inexorably growing in the last few years. The increasing use of fossil fuels in vehicles is causing serious problems to the environment in populated zones due to the gaseous emissions. This fact has produced a global movement towards trying to find more environmentally friendly energy resources, among which hydrogen constitutes a cleaner one [1,2].

The hydrogen which feeds the PEM fuel cells is generally obtained by the reforming of hydrocarbons or alcohols. In general, this step is followed by the Water Gas Shift reaction, where the H_2 content is increased and the CO concentration is reduced around 1%. However, it is necessary that the CO content in the hydrogen-rich stream be less than 10 ppm in order to avoid damaging the anode of the cell.

In this sense, the CO Preferential Oxidation (COPrOx) reaction is a widely studied alternative to eliminate CO in the hydrogen-rich stream almost completely without consuming H_2 [3,4]. Several authors have developed successful catalysts based on precious or noble metals, achieving excellent results [5–8], but the elevated cost of these materials have led researchers to investigate other alternatives based on low-cost materials.

Numerous articles on transition metal-ceria systems have been published, in which CeO_2 plays a fundamental role in redox reactions due to its easiness to release and store oxygen.

* *Corresponding author*. Tel.: +54 342 4536861.
E-mail address: aboix@fiq.unl.edu.ar (A.V. Boix).
http://dx.doi.org/10.1016/j.ijhydene.2016.01.099

Likewise, the CuO–CeO_2 system has also been widely studied by several authors and the results obtained in COPrOx are comparable to those reached by noble catalysts on a great number of occasions [9–11]. In our previous studies, we found that Co_3O_4 based catalysts were active and selective for the preferential CO oxidation in rich H_2 stream [12,13].

However, it is still a matter of considerable debate how cerium influences catalytic processes, particularly the role of the redox couple Ce^{4+}/Ce^{3+} and the ability to store and release oxygen under clearly reducing conditions. Special attention is given to the role of lattice vacancies in CeO_2, and CeO-based mixed oxides and how these affect the catalytic chemistry, as well as the effects on catalysts arising from the occurrence of metal-ceria interactions.

In this vein, Raman spectroscopy is a powerful catalytic characterization technique to study the molecular structure of supported metal oxide catalysts. Furthermore, Raman spectroscopy can provide this information under *in situ* reaction conditions (temperature, partial pressure of gas phase components, etc.) [14].

The combination of fundamental molecular structural information and *in situ* characterizations allows the development of the molecular-level understanding of structure-activity/selectivity relationships for catalytic reactions.

In the present work, cobalt-based catalysts prepared by the wet impregnation or co-precipitation method using ZrO_2 and CeO_2 as the supports were studied by Raman *in situ* under the same reaction conditions used for the catalytic evaluation in the preferential oxidation of CO. These two supports were chosen in order to compare the behavior of a relatively inert support (ZrO_2) with another support with redox properties (CeO_2). Characterization by temperature programmed reduction (TPR) and X-ray photoelectron spectroscopy (XPS) were carried out to complete the study.

Experimental

Preparation of catalysts

Firstly, CeO_2 particles were prepared by the co-precipitation method. In this case, a $NH_4(OH)$ solution was added drop by drop to a vessel which contained a solution of $Ce(NO_3)_2$, and then, the mixture was kept under continuous stirring during 2 h. Afterwards, the precipitate was filtered, washed and dried at 120 °C overnight. Then, the powder was calcined in air flow at 370 °C during 5 h [13].

After that, a cobalt-based catalyst with c.a. 10 wt.% was prepared by the wet impregnation method and denoted as CoCe(WI). For this purpose, an aqueous solution of $Co(NO_3)_2$ was added to a vessel which contained the CeO_2 powder previously prepared. The mixture was evaporated under continuous agitation at 70 °C until achieving a paste, which was dried at 120 °C in an oven overnight.

With the aim of comparing different preparation methods, a catalyst with a similar content of cobalt was obtained by means of the co-precipitation method, CoCe(CP). The procedure was carried out by adding $NH_4(OH)$ drop by drop into a solution of Co and Ce nitrates under vigorous stirring. The resulting precipitate was filtered and washed several times with distilled water, and then it was dried in an oven overnight [13]. Finally, a Co/ZrO_2 catalyst was prepared by the wet impregnation method with c.a. 10 wt. % cobalt on ZrO_2 in order to study a different support. A commercial monoclinic ZrO_2 of low surface area (6.8 $m^2\ g^{-1}$) was mixed with an aqueous solution of $Co(NO_3)_2$. Then similar stages of evaporation and drying were followed. The resulting catalyst was denominated CoZ(WI) [12]. All catalysts were calcined for 4 h at 450 °C under air flow.

Catalytic tests

CO preferential oxidation experiments were performed in a fixed-bed flow reactor at atmospheric pressure. Powder samples (200 mg) were placed in a tubular quartz reactor (8 mm i.d.). The reaction mixture consisted of CO 1%, O_2 1% and H_2 40%, He balance. The flow gas rate was 95 $cm^3 \cdot min^{-1}$.

The CO conversion and the selectivity towards CO_2 were defined as:

$$C_{CO} = 100 \cdot (1 - [CO]/[CO]^{\circ})$$

$$S = 100 \cdot [CO_2]/2 \cdot ([O_2]^{\circ} - [O_2])$$

where [CO], [CO_2] and [O_2] are reactor exit concentrations and [CO]°, [O_2]° represent feed concentrations, which were measured with a GC-2014 Shimadzu chromatograph equipped with a TCD cell. All the catalysts were pretreated during 30 min in a 10% O_2/He mixture at 200 °C before the catalytic test.

Catalyst characterization

Chemical composition determinations

Elemental analyses of catalysts were performed by inductively coupled plasma atomic emission spectroscopy (ICP-AES) on an ICP-OPTIMA 2100 DV Perkin Elmer instrument.

X-ray diffraction (XRD)

The patterns of catalysts were measured on a Philips PW 1710/01 Instrument. The measurements were performed with CuKα radiation (graphite monochromator, 40 kV and 30 mA) in a range of $2\theta = 10°–80°$, with a step size of 0.02° and 3 s for each step. The peaks observed for the catalysts were compared to standards published by JCPDS data [15].

Transmission electronic microscopy (TEM)

The TEM analyses were carried out using FEIR transmission electron microscope, Tecnai T20 model with an electron source of 200 kV.

Laser Raman spectroscopy

The Raman spectra of calcined powders were recorded using a LabRam spectrometer (Horiba-Jobin-Yvon) coupled to an Olympus confocal microscope (a 100X objective lens was used for simultaneous illumination and collection), equipped with a CCD detector cooled to about 200 K using the Peltier effect. The excitation wavelength was in all cases 532 nm (Spectra

Physics diode pump solid state laser). The laser power was set at 30 mW.

In situ LRS measurements were performed on a Linkam high temperature cell. The powder catalysts were placed in the cell and the reactant gases flowed through the sample. The gas feed mixture was composed of CO, O_2, H_2 and N_2 in similar concentrations which were used in COPrOx experiments when the fixed-bed reactor was used. Firstly, the catalyst was oxidized in the LR cell under an O_2/N_2 flow at 200 °C during 30 min. After that, it was cooled in an inert atmosphere. The spectra were registered under COPrOx conditions at different temperatures. First, a spectrum was recorded at room temperature. Then, the temperature was increased until a value close to the temperature where the maximum CO conversion was obtained in COPrOx experiments, in order to notice any change in the catalysts structure. After that, the temperature was increased from 200 to 450 °C, the spectra were recorded every 50 °C, and the sample held several minutes at each temperature in order to reach steady state.

Temperature-programmed reduction

H_2-TPR experiments were performed with an OKHURA TP-2002S instrument equipped with a TCD detector on samples of 100 mg in a 5%H_2/Ar gas mixture using a temperature ramp rate of 10 °C·min^{-1}. Prior to the TPR analysis, the samples were treated at 300 °C for 30 min under N_2 flow to clean the surface.

X-ray photoelectron spectroscopy

XPS analyses were performed using a multi-technique system (SPECS) equipped with a dual Mg/Al X-ray source and a hemispherical PHOIBOS 150 analyzer operating in the fixed analyzer transmission (FAT) mode. The spectra were obtained with a pass energy of 30 eV, and the AlKα X-ray source ($h\nu = 1486.6$ eV) was operated at 100 W. The working pressure in the analyzing chamber was less than 5.9×10^{-7} Pa. The spectra regions corresponding to Co 2p, O 1s and Ce 3d core levels were recorded. All photoelectron binding energies were referenced to the C1s peak of adventitious carbon, set at 284.6 eV.

Firstly, the CoCe(WI) catalyst was measured in calcined state. Then, it was reduced *in situ* at 350 °C in the reaction chamber of the spectrometer by a 5% H_2/Ar stream, and then measured. Finally, the catalyst was reoxidized at 170 °C in the reaction chamber by an 5%O_2/Ar stream and then measured. The data treatment was performed with the Casa XPS program (Casa Software Ltda., UK).

Results and discussion

Chemical and structural characterization

The elemental composition of the three cobalt-based catalysts was determined by means of the ICP technique and the cobalt content resulted 10.6, 8.6 and 9.2 Co wt.% for CoCe(WI), CoCe(CP) and CoZ(WI), respectively.

The structure of the different Co-supported catalysts as well as that of the CeO_2 support was analyzed by means of XRD. Fig. 1 shows the diffraction patterns of the powders. The Co/CeO_2 particles show a pattern dominated by the CeO_2 diffraction peaks, whose main peaks appear at $2\theta = 28.59$, 47.52, 56.38, 33.11° (34–0394). The peaks of Co_3O_4 at $2\theta = 36.88$, 31.30, 65.29, 59.41 and 44.85° do not seem to modify the structure of the CeO_2 diffraction pattern, so it is probable that the cobalt species do not insert in the lattice of the ceria. It should be noted that the cobalt peaks pertaining to the impregnated sample are more intense than those of the co-precipitated one. On the other hand, the diffraction pattern of CoZ(WI) catalysts shows the peaks associated with the monoclinic ZrO_2, and the main signal of Co_3O_4 at $2\theta = 36.8$° can also be observed.

According to Scherrer's equation, the average sizes of the crystallite calculated with the main peak of CeO_2 phase for CoCe(WI) and CoCe(CP) resulted 8.9 and 8.6 nm respectively, whereas for the Co_3O_4 phase, the average particle sizes were 31.2 and 14.5 nm, respectively.

In addition, the particles supported on ceria were analyzed by transmission electronic microscopy in order to determine the shape and the particle size. Fig. 2(A) and (B) shows that both CoCe(WI) and CoCe(CP) present spherical shape and the mean particle size resulted about 8.9 ± 1.6 nm and 7.3 ± 2.0 nm, respectively which is in agreement with values calculated from XRD data. In spite of the fact that the CoCe(WI) and CoCe(CP) catalysts were synthesized by two different methods, the results show that both particle size and

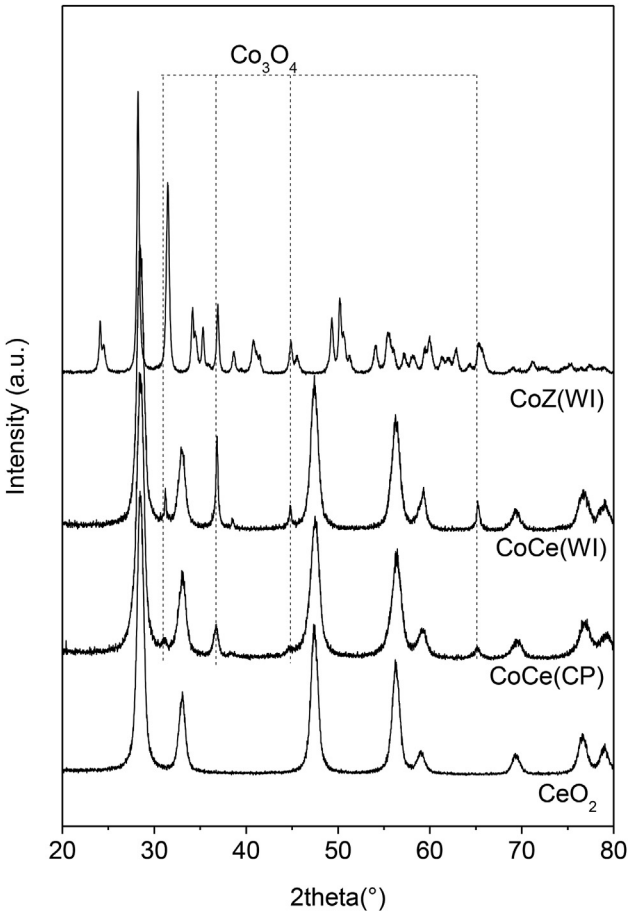

Fig. 1 – XRD patterns of CoCe(CP), CoCe(WI) and CoZ(WI) catalysts and CeO_2 support.

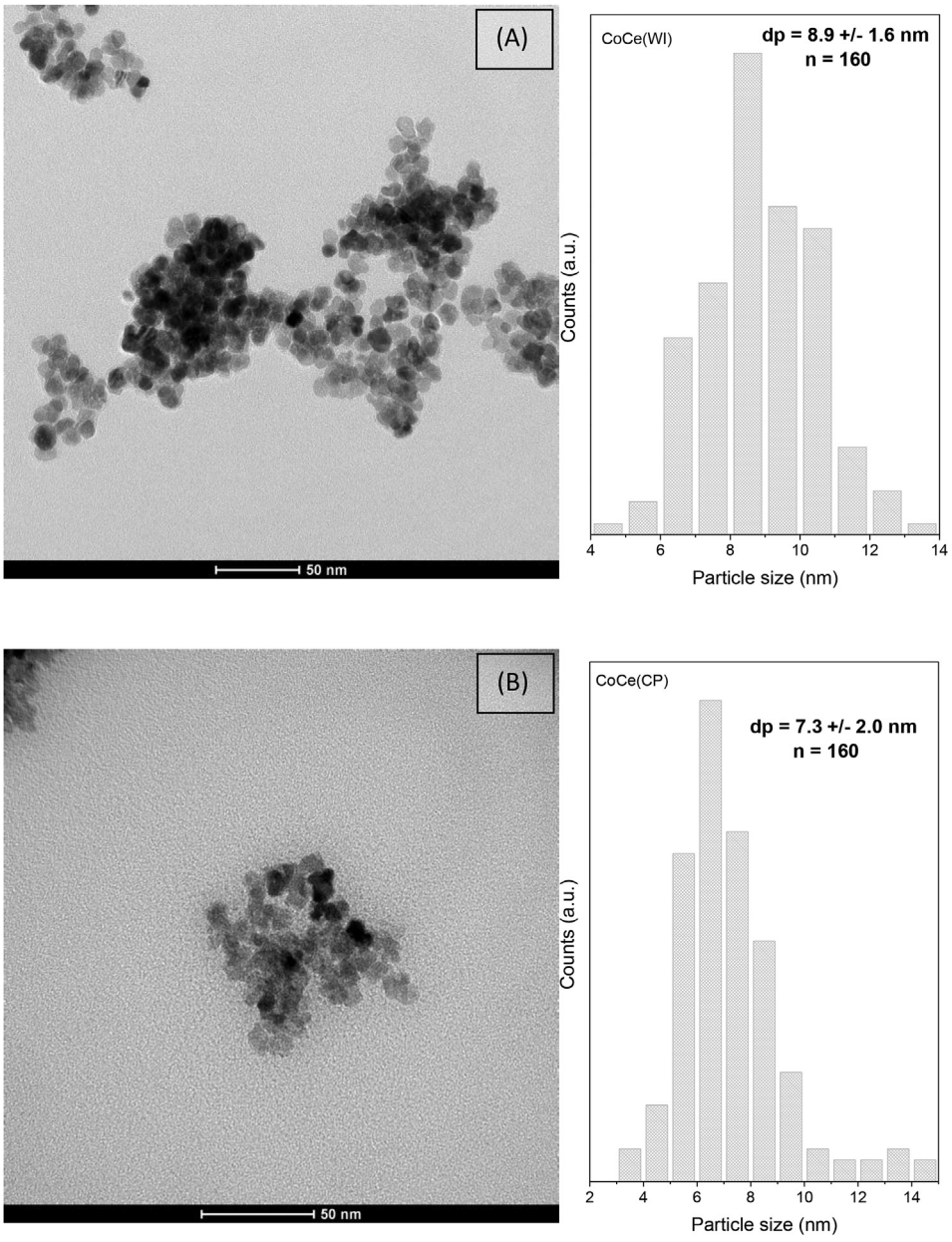

Fig. 2 – TEM images and size distribution graphic of (A) CoCe(WI) and (B) CoCe(CP).

shape were similar. The CoZ(WI) particles were also analyzed by means of TEM (not shown), they present irregular shape and a high dispersion in their sizes.

Raman in situ

Firstly, the CeO_2 support was characterized by Raman spectroscopy under the same reaction conditions as was previously analyzed in a fixed-bed reactor. In this vein, the CeO_2 showed low CO conversion, 12–55% (between 100 and 200 °C), and a maximum of 83% at 250 °C.

Fig. 3(A) shows CeO_2 spectra recorded at different temperatures. The first spectrum was registered at room temperature. It consisted of a main band at 464 cm^{-1}, which belongs to the F2g mode of the CeO_2. The spectrum also shows other weaker signals at 259, 587, and 1173 cm^{-1} which are assigned as the second order 2 TA, D and 2TO Raman modes, respectively [16,17] and they are strongly related to oxygen vacancies in the ceria structure. Moreover, a weak band at 1050 cm^{-1} is associated with the creation of oxygen defect sites and to the stretching mode related to the terminal Ce=O [18].

Then, the sample was maintained at 160 °C under reaction flow during 60 min with the aim to identify any possible change due to the chemical reaction. This temperature is related to the maximum conversion previously reached by the Co/CeO_2 catalysts in the fixed-bed reactor. Although at this temperature the CO conversion resulted 25% for the CeO_2 sample, the Co/CeO_2 catalysts reached almost 100%.

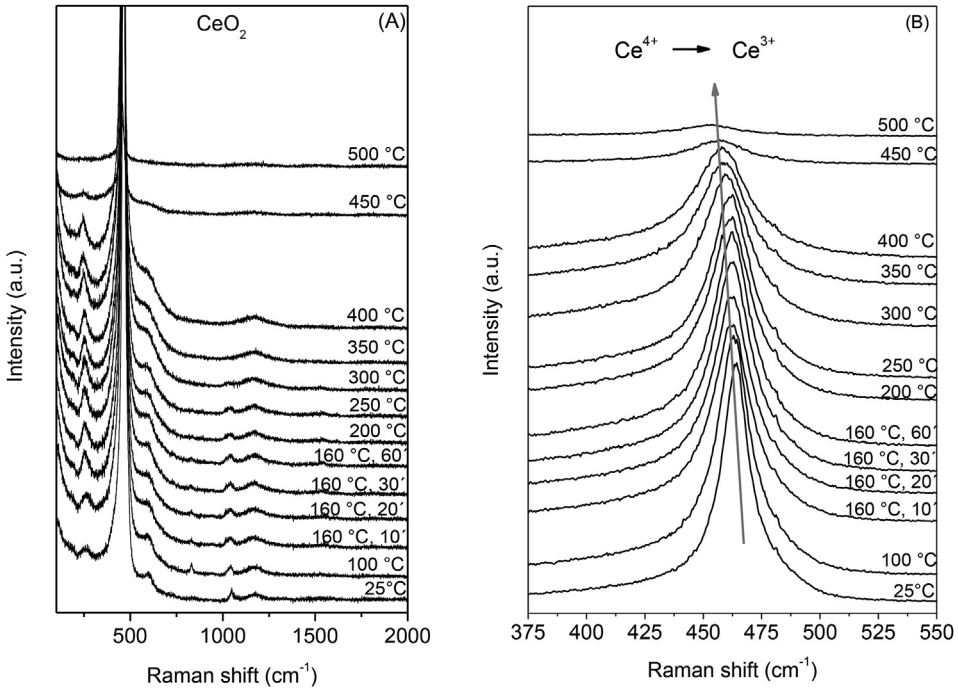

Fig. 3 – (A) In situ Raman spectra of CeO_2 support at different temperatures, under reaction conditions: 1% CO, 1% O_2 and 40% H_2 in inert stream. (B) Enlargement of main CeO_2 peaks zone at different temperatures.

After that period, no appreciable modification in the intensity of the signals was detected and only a shift of the main peak towards a lower wavenumber was observed. Fig. 3(B) shows an enlarged zone corresponding to the main peak of CeO_2 and it is possible to observe the peak shift in detail.

After that, the temperature was increased and the recording of the spectra was carried out at 200, 250, 300, 350, 400 and 450 °C. The spectrum measured at 250 °C also showed a shift of the main signal of the CeO_2 at 459 cm^{-1}.

Then, as the temperature continued increasing, the spectra recorded at 300 and 350 °C showed the same Raman signals at 459, 259, 587, and 1173 cm^{-1}, but at 400 °C the bands at 259, 587 and 1173 cm^{-1} were weaker, while at 450 and 500 °C, the bands at 259 and 1173 cm^{-3} were almost undetectable.

The position of the main peak moved from 464 cm^{-1} to 454 cm^{-1} and the peak width increased with rising temperature from 25 °C to 500 °C under reaction conditions. Smaller peaks near 259, 587, 1050 and 1173 cm^{-1} depended on temperature but to a lesser extent.

The shift in Raman signal of 4–5 cm^{-1} could be due to thermal expansion as well as to phonon coupling and decay [19]. In agreement with Lee et al. [18], the additional downward shift is mostly due to the lattice expansion and mode softening that occurs when oxygen vacancies are created from the oxidation of CO, which leads to two Ce^{+3} ions (ionic radius 1.143 A) replacing two Ce^{+4} ions (0.970 A) for each oxygen vacancy created [19].

$$2Ce^{4+} + CO + O^{2-} \rightarrow 2Ce^{3+} + CO_2 + Vo \text{ (oxygen vacancy)}$$

Afterwards, as described in the Experimental section, Co/CeO_2 catalysts were prepared both by the co-precipitation and wet impregnation methods. In both catalysts, the CO conversion was by far higher than the CO conversion reached by CeO_2, even at lower temperature.

When the CoCe(CP) was analyzed by the *in situ* Raman technique, the main signal of CeO_2 at 464 cm^{-1} as well as the signals associated with Co_3O_4 were detected at room temperature, and they are shown in Fig. 4(A). The bands corresponding to Co_3O_4 at 195, 523 and 621 cm^{-1} were attributed to the F2g mode, while the peaks at 481 and 685 cm^{-1} were assigned to the Eg and A1g modes, respectively [20]. Moreover, two broad, very weak signals were detected at 500–600 cm^{-1} and 1100–1200 cm^{-1}, which were ascribed to oxygen vacancies of the CeO_2 structure. On the other hand, Vuurman et al. assigned the broad signal between 500 and 600 cm^{-1} to CoO dispersed over the surface of alumina support [21].

Next spectra were recorded at 155 °C during 3 h because this temperature value is close to the temperature at which this catalyst reached the highest CO conversion. Fig. 4(B) shows that this catalyst reached 99% of CO conversion at 165 °C.

After 3 h of reaction, the most important change detected is a slight shift of the main signal of the CeO_2 toward a lower wavenumber. This peak shift was also observed in the spectra recorded at 200 °C and 250 °C.

At 300 °C, the signal associated with CeO_2 and Co_3O_4 were still present, but the intensity of the Co_3O_4 signals showed a decrease in comparison to the spectra recorded at lower temperature. When the temperature reached 350 °C, the bands belonging to Co_3O_4 were almost undetected. However, the signals at 500–600 cm^{-1} could be still distinguished and the main signal of CeO_2 was shifted to a lower wavenumber (at 453 cm^{-1}).

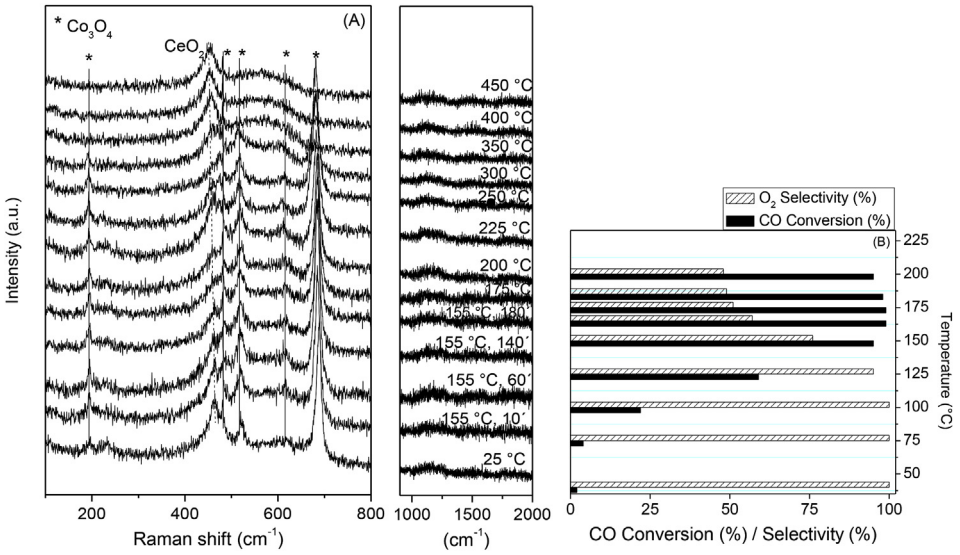

Fig. 4 – (A) In situ Raman spectra of the CoCe(CP) catalyst at different temperatures, under reaction conditions: 1% CO, 1% O_2, 40% H_2, in inert stream. (B) CO conversion and selectivity bars of the COPrOx reaction carried out in a fixed-bed reactor.

At 450 and 500 °C, the only detected signals were the main CeO_2 peak and the broad signal at 500–600 cm^{-1} associated with oxygen vacancies. In addition, by TPR results it was possible to confirm that Co_3O_4 species are completely reduced above 450 °C.

The CoCe(WI) catalyst prepared by wet impregnation method was also analyzed by means of Raman *in situ* with a similar procedure as the one used with the previous catalyst. Fig. 5(A) shows the spectra recorded at different temperatures, whereas Fig. 5(B) shows the CO conversion and O_2 selectivity toward CO_2. These figures show that both the spectroscopic and the catalytic results from this catalyst are very close to the results obtained by the catalyst prepared by the co-precipitation method.

The spectrum which was measured at room temperature showed the main signal of the CeO_2 at 464 cm^{-1}, as well as the Co_3O_4 bands at 196, 480, 522, 620 and 688 cm^{-1}. Also two broad signals were detected at 500–600 cm^{-1} and 1100–1200 cm^{-1}. After that, the temperature was increased at 165 °C and several spectra were recorded during 3 h. This catalyst reached its maximum CO conversion at 175 °C, so it was interesting to analyze a possible change in the catalyst during the chemical reaction.

Fig. 5(A) shows that the intensity of Co_3O_4 bands and the main CeO_2 band remained constant after 3 h of reaction. This stability of the active centers is in agreement with the catalytic stability tested for us in a previous work, where Co/CeO_2 catalysts were stable after 100 h of time-on-stream [13].

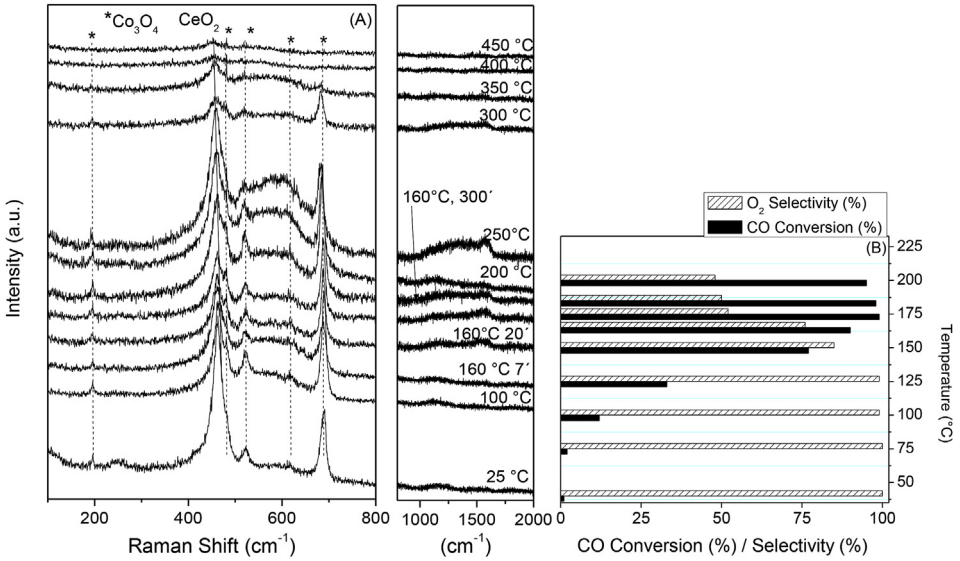

Fig. 5 – (A) In situ Raman spectra of the CoCe(WI) catalyst at different temperatures, under reaction conditions: 1% CO, 1% O_2, 40% H_2, in inert stream. (B) CO conversion and selectivity bars of the COPrOx reaction carried out in a fixed-bed reactor.

However, the slight increasing of the band at 500–600 cm^{-1} could suggest a change of the oxygen vacancies.

After that, the spectra measured at 200, 250 and 300 °C did not show significant changes as compared with the previously recorded spectra, although a little decrease of the intensity of the main CeO_2 signal and an increase in the band between 500 and 600 cm^{-1} were observed.

When the temperature reached 350 °C, the intensity of the Co_3O_4 signals started to decrease, and at 450 °C these bands completely disappeared. Only the main band of CeO_2 at 456 cm^{-1} could be detected, which indicates that the cobalt species were completely reduced.

Despite the different preparation methods used, both Co/CeO_2 catalysts showed very similar catalytic results, as the Raman spectra recorded under COPrOx conditions. It has been observed in Figs. 4(B) and 5(B) that the catalysts prepared by the co-precipitation method are a bit more active than the catalyst prepared by wet impregnation. As a matter of fact, Co Ce(CP) reached the maximum conversion (99%) at 165 °C, while the maximum reached by CoCe(WI) (99%) was a bit higher temperature, 175 °C. This fact could be related to a greater interaction between the cobalt and cerium species, which are benefited by the preparation method.

On the other hand, it can be observed that in both Co/CeO_2 catalysts the Raman spectra corresponding to the active species (Co_3O_4) remained stable during the temperature interval at which they showed the highest activity. However, a very little difference was found, particularly at 200 and 250 °C, where a more pronounced band at 500–600 cm^{-1} in the CoCe(WI) than in CoCe(CP) was observed. In this way, the small difference in this band assigned to oxygen vacancies (see above) is not enough to produce an activity improvement.

In this vein, for this kind of catalysts composed by a transition metal oxide like Co_3O_4 in contact with cerium oxide, it has been proposed that they follow a Mars van Krevelen mechanism for the COPrOx reaction. For CuCeOx catalysts, it has been accepted that both CO and H_2 oxidation reactions involving molecular oxygen over metal oxide catalysts proceed by a redox mechanism [22]. Thus, it is possible that CoCeOx catalysts also have these characteristics.

For CO and H_2 oxidation, the following reactions could be written:

$$Co_3O_4 + CO \rightarrow 3CoO + CO_2$$

$$Co_3O_4 + H_2 \rightarrow 3CoO + H_2O$$

While, the reoxidation of reduced cobalt oxide is written as:

$$3CoO + 2CeO_2 \rightarrow Co_3O_4 + Ce_2O_3$$

In this process, the Co^{2+} species are always re-oxidized by the Ce^{4+} species which are in contact with Co^{2+} and, therefore, the Ce^{4+} species are reduced to Ce^{3+}. Finally, the Ce_2O_3 formed during the re-oxidation of CoO, is later re-oxidized to CeO_2 by O_2 from the gas phase.

As a consequence, a permanent equilibrium is established:

$$Ce^{4+} + Co^{2+} \leftrightarrow Ce^{3+} + Co^{3+}$$

This equilibrium acts as a buffer effect by which Co^{3+}, which is the active species in this reaction, is always present, even in a reducing atmosphere.

Finally, a 9.2 wt. % cobalt catalyst prepared by wet impregnation over ZrO_2 was studied by Raman *in situ* in order to analyze another kind of support, which has no redox properties under the reaction temperature range. Fig. 6(A) shows the spectra recorded at different temperatures, while Fig. 6(B) shows the CO conversion and O_2 selectivity, previously obtained with a fixed-bed reactor. This catalyst was less active than the Co10Ce catalysts previously analyzed. It reached the higher CO conversion (89%) at a 200 °C, which is a temperature rather higher than the maximum CO conversion temperature for Co10Ce catalysts.

At room temperature, the spectra show the bands associated with Co_3O_4 as well as those of monoclinic ZrO_2. The main ZrO_2 bands appeared at 179 and 192 and 476 cm^{-1}, which were overlapped with Co_3O_4 bands. Another support signals at 334, 504, 560 and 580 cm^{-1} were also detected.

Then, the temperature was increased at 190 °C, which is a value close to the temperature of higher conversion for this catalyst and it was maintained at this value during 3 h in order to study any change during the reaction. However, any appreciable change in the intensity of the signals was detected.

When the temperature increased up to 300 °C, the intensity of the bands remained stable. At 350 °C, it was possible to observe a partial decrease of the intensity of Co_3O_4 bands, which indicate that these species are reduced to some extent due to the increase of temperature in a high hydrogen concentration environment. At 400 °C, the Co_3O_4 bands completely disappeared and only the main signals of the ZrO_2 were observed.

It should be noted that the highest CO conversion is reached at a temperature value in which the reduction of the cobalt species have not yet been detected in any of the catalysts studied.

In this sense, Fig. 7 shows TPR experiments were carried out for Co/CeO_2 and CoZ(WI) catalysts. It can be seen that the reduction of the Co_3O_4 species started around 250 °C and it is completed close to 450 °C. In agreement, when the Raman spectra measured under reaction conditions, the intensity of the signals corresponding to the Co_3O_4 species started to decrease at 350 °C for all catalysts and they disappeared at 450 °C completely. These results suggest that at temperatures between 250 °C and 350 °C, both CO and hydrogen are able to reduce the Co_3O_4 species, yielding CO_2, H_2O as products, and CoO and Co° species.

Under steady-state reaction conditions, the small amount of oxygen present (1%) is enough to quickly reoxidize these reduced species, thus restoring Co_3O_4, since only Co_3O_4 is detected by *in situ* Raman measurements. In order to support this result, others *in situ* Raman experiments with CoCe(WI) catalyst were carried out. More details can be seen in the Supplementary Data Section. First of all the calcined was

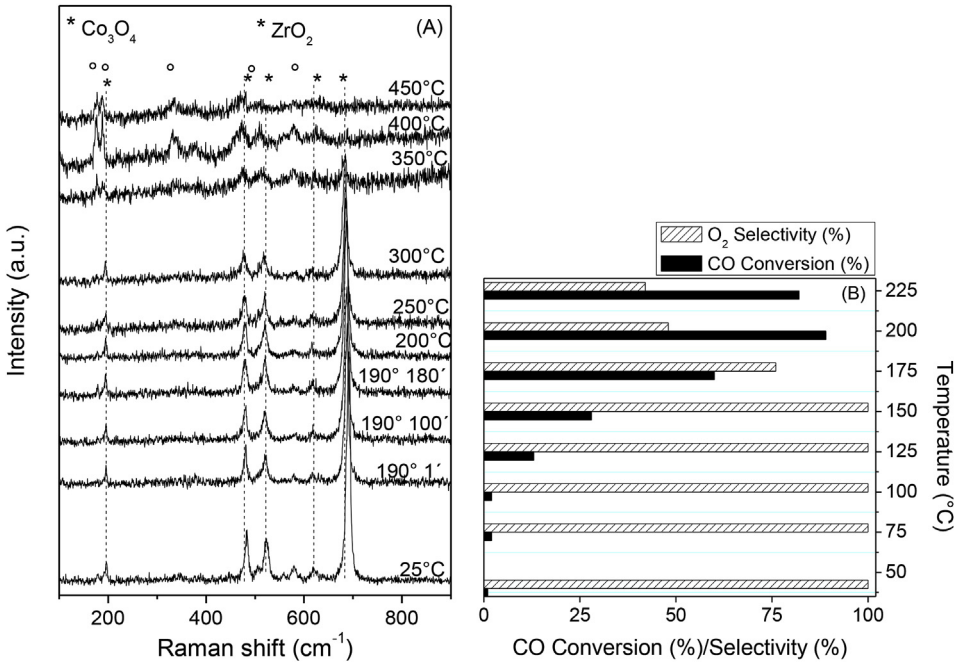

Fig. 6 – (A) In situ Raman spectra of the CoZ(WI) catalyst at different temperatures, under reaction conditions: 1% CO, 1% O_2, 40% H_2, in inert stream. (B) CO conversion and selectivity bars of the COPrOx reaction carried out in a fixed-bed reactor.

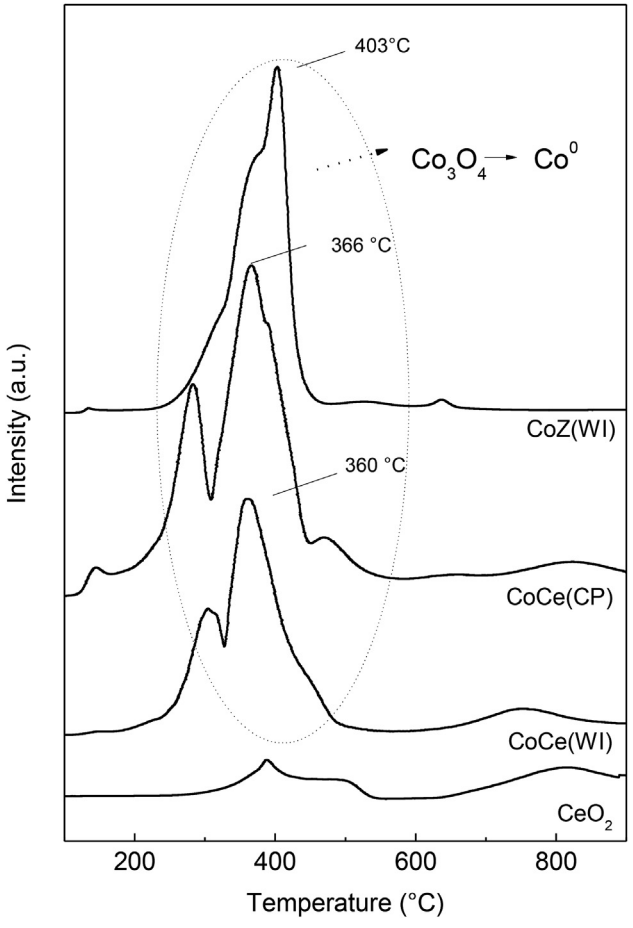

Fig. 7 – Temperature-programmed reduction of CoCe(CP), CoCe(WI) and CoZ(WI) catalysts and CeO_2 support.

exposed to reducing stream (1% CO/Ar). The Fig. S1(A) shown that the cobalt species of the catalyst were completely reduced at 325 °C. Then, the sample was treated with an oxidizing stream (1% O_2/Ar), where it can be clearly seen at 200 °C the reoxidation of reduced cobalt species to Co_3O_4 (Fig. S1(B)). After that, the catalyst was again reduced by a reducing stream (1% CO and 40% H_2 in Ar) at 350 °C and then, it was cooled at room temperature. Finally, the catalyst was treated with COPrOx gaseous reactants (1% CO, 1% O_2, 40% H_2 in Ar). I was possible to observe at 150 °C the bands corresponding to Co_3O_4 species, which means the catalyst was reoxidized (Fig. S1(C)).

This result suggests that the redox mechanism probably proceeds for the catalyst studied in this work, in which the reduction step limits the overall reaction and the re-oxidation of the surface being very fast.

In addition, the surface species of CoCe(WI) catalyst were analyzed by means of XPS after being exposed to different *in situ* treatments. Fig. 8(A) shows the Co2p spectral region corresponding to calcined and after-treated sample under reducing (H_2/Ar at 350 °C) and reoxidizing (O_2/He 170 °C) streams.

In the calcined sample, the Co $2p_{3/2}$ peak position was found around 780.0 ± 0.1 eV, with a spin–orbit splitting at 795.0 eV corresponding to the Co $2p_{1/2}$ peak. The binding energy of the main peak correspond to either Co^{2+} or Co^{3+} species of Co_3O_4 phase, since binding energy differences are negligible for both oxidation states. Also, it is known that the XP spectrum exhibits a satellite peak for Co^{2+} component, on the high energy binding energy side of the main peak [12,13].

In the spectra corresponding to the reduced sample, the main peak of Co $2p_{3/2}$ can be observed at 777.6 ± 0.1 eV which correspond to metallic Co. Moreover, it is possible to identify

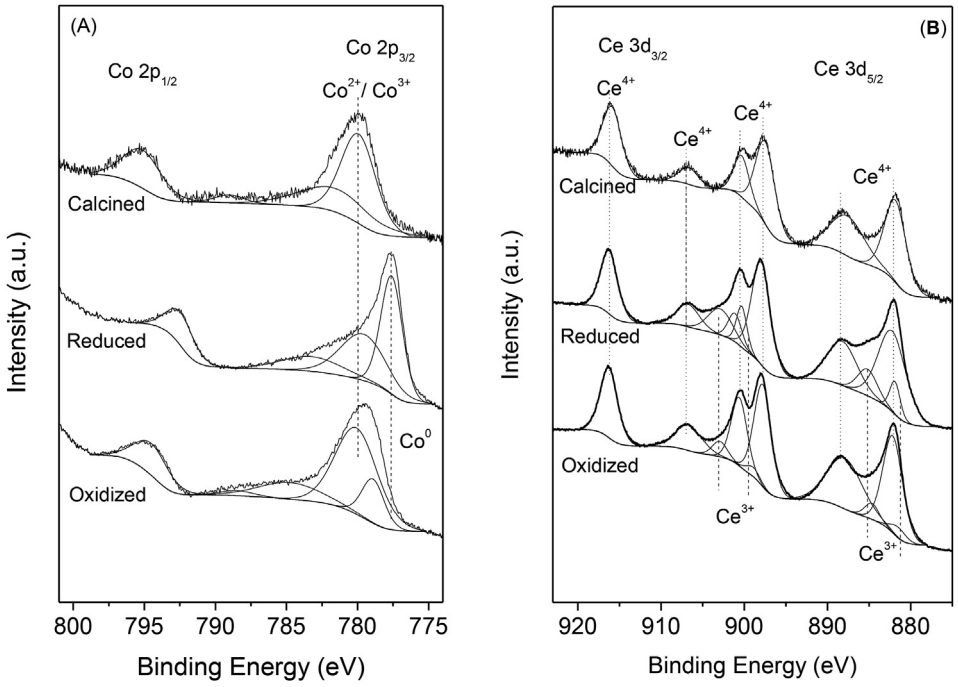

Fig. 8 – XP spectra of CoCe(WI) catalyst, Co 2p (A) and Ce 3d (B) regions.

another component at 779.6 eV belong to cobalt oxide. In contrast, when the catalyst was re-oxidized at 170 °C, the spectrum shows a change. The peak intensity associated with metallic Co decreased while the peak at 780.1 eV increased, indicating a fast reoxidation of the cobalt species, even at low temperature.

The CoCe(WI) Ce 3d spectra corresponding to the calcined, *in situ* reduced at 350 °C and reoxidized at 170 °C sample are depicted in Fig. 8(B).

The spectra of the Ce 3d region show signals with binding energies at 882.0, 888.3 and 897.7 eV, which correspond to the $Ce3d_{5/2}$ core level and peaks at 900.4, 906.9 and 916.2 eV, which belong to the Ce $3d_{3/2}$ level. These B.E. values are characteristic of Ce^{4+} species [13]. In addition, peaks corresponding to Ce^{3+} species were found at 881.7, 885.2, 899.5 and 903.0 eV after reducing treatment. Finally, the re-oxidation treatment at 170 °C decreased the intensities of signals associated to Ce^{3+} component, indicating that a reoxidation process occurred.

The results observed by XPS are agreement with the re-oxidation proposed in the Mars Van Krevelen mechanism at the reaction temperature, where the CO conversion reaches its maximum at 165 °C.

In brief, CoZ(WI) resulted less active than the Co10Ce catalysts. The higher performance of the $CoCeO_2$ catalysts compared to the CoZ(WI) catalysts could be related to two reasons(could be explained by two possible reasons): i) the buffer equilibrium mentioned above, which always provides Co_3O_4 species; ii) the oxygen vacancies which were originally present and were also created in the ceria during the reaction.

In the redox mechanism postulated for $CoCeO_2$ catalysts, vacancies are created when either CO_2 or H_2O are desorbed from the catalyst surface. These vacancies are then filled by oxygen from the gas phase and, simultaneously, the reduced cations are re-oxidized. The oxygen which fills the vacancy could also be transported through the lattice of the ceria.

These facts which occur in the $CoCeO_2$ catalysts allow a better catalytic performance with respect to the CoZ(WI) catalyst.

In addition, in TPR experiments it has been mentioned that the reduction of Co_3O_4 started around 250 °C in the three catalysts, but the reduction profile of $CoCeO_2$ and CoZ(WI) presents some differences. While the $CoCeO_2$ catalysts showed two reduction peaks associated with two stages of reductions (Co_3O_4/CoO and CoO/Co^0), the CoZ(WI) catalyst showed only one reduction peak, whose maximum is at a bit higher temperature. This could be explained due to the fact that the presence of oxygen vacancies enhances the reduction of Co_3O_4, whereas ZrO_2 does not interact with the active phase. In the same way, CeO_2 is more able to reduce Co_3O_4 in a reducing stream. It is also more able to oxidize the reduced CoO species which are produced during the chemical reaction due to CO_2 and H_2O production.

Conclusions

The reaction atmosphere during the COPrOx reaction, in contact with the surface of Co/CeO_2 and Co/ZrO_2 catalysts provokes changes in the species present that can be effectively studied with the *in situ* Raman spectroscopy. These changes occur not only in the Co active species, but also in the CeO_2 support, but not in the case of ZrO_2. A Raman shift of the CeO_2 main peak is observed when increasing the temperature, which could be related to CeO_2 surface reduction,

accompanied by the lattice expansion that occurs when oxygen vacancies are created from the oxidation of CO.

CoCe(CP) and CoCe(WI) catalysts showed very similar Raman spectra under COPrOx conditions despite using different preparation methods, in agreement with the catalytic activity shown by both catalysts. The maximum CO conversion (99%) on the Co Ce(CP) catalyst was at 165 °C, while on the CoCe(WI) was at bit higher temperature (175 °C). This fact could be related to a greater interaction between the cobalt and cerium species, which are benefited by the preparation method.

In situ Raman and XP spectroscopies show that the redox mechanism occurs on the Co/CeO_2 catalysts, where the reduction step limits the overall reaction and the re-oxidation of the surface is very fast.

On the other hand, the CeO_2 support is better than the ZrO_2 one because the former accelerates the surface exchange between reduced and oxidized species due to the high mobility of surface lattice oxygen and the presence of oxygen vacancies. The $Ce^{4+} + Co^{2+} \leftrightarrow Ce^{3+} + Co^{3+}$ process acts as a buffer effect by which Co^{3+}, which is the active species in this reaction, is always present even in a reducing atmosphere, as seen by *in situ* Raman characterization.

Acknowledgments

The authors acknowledge the financial support received from UNL, ANPCyT and CONICET.

Thanks are given to Nadia Gamba for her technical assistance, and to Fernanda Mori for the XPS measurements.

Appendix A. Supplementary data

Supplementary data related to this article can be found at http://dx.doi.org/10.1016/j.ijhydene.2016.01.099.

REFERENCES

[1] Wang W, Tade MO, Shao Z. Research progress of perovskite materials in photocatalysis- and photovoltaics-related energy conversion and environmental treatment. Chem Soc Rev 2015;44:5371–408.
[2] Jiao Y, Zheng Y, Jaroniec M, Qiao SZ. Design of electrocatalysts for oxygen- and hydrogen-involving energy conversion reactions. Chem Soc Rev 2015;44:2060–86.
[3] Bion N, Epron F, Moreno M, Mariño F, Duprez D. Preferential oxidation of carbon monoxide in the presence of hydrogen (PROX) over noble metals and transition metal oxides: advantages and drawbacks. Top Catal 2008;51:76–88.
[4] Park ED, Lee D, Lee HC. Recent progress in selective CO removal in a H_2-rich stream. Catal Today 2009;139:280–90.
[5] Liu K, Wang A, Zhang T. Recent advances in preferential oxidation of CO reaction over Platinum group metal catalysts. ACS Catal 2012;2:1165–78.
[6] Komatsu T, Takasaki M, Ozawa K, Furukawa S, Muramatsu A. PtCu intermetallic compound supported on alumina active for preferential oxidation of CO in hydrogen. J Phys Chem C 2013;117:10483–91.
[7] Li X, Soon Fang SS, Teo J, Foo YL, Borgna A, Lin M, et al. Activation and deactivation of Au–Cu/SBA-15 catalyst for preferential oxidation of CO in H_2-rich gas. ACS Catal 2012;2:360–9.
[8] Kipnis M, Volnina E. New approaches to preferential CO oxidation over noble metals. Appl Catal B Environ 2010;98:193–203.
[9] Martínez-Arias A, Gamarra D, Fernández-García M, Hornés A, Bera P, Koppány Z, et al. Redox-catalytic correlations in oxidised copper-ceria CO-PROX catalysts. Catal Today 2009;143:211–7.
[10] Zeng S, Zhang W, Sliwa M, Su H. Comparative study of CeO_2/CuO and CuO/CeO_2 catalysts on catalytic performance for preferential CO oxidation. Int J Hydrogen Energy 2013;38:3597–605.
[11] Meng M, Liu Y, Sun Z, Zhang L, Wang X. Synthesis of highly-dispersed $CuO\text{-}CeO_2$ catalyst through a chemisorption-hydrolysis route for CO preferential oxidation in H_2-rich stream. Int J Hydrogen Energy 2012;37:14133–42.
[12] Gómez LE, Tiscornia IS, Boix AV, Miró EE. Co/ZrO_2 catalysts coated on cordierite monoliths for CO preferential oxidation. Appl Catal A General 2011;401:124–33.
[13] Gómez LE, Tiscornia IS, Boix AV, Miró EE. CO preferential oxidation on cordierite monoliths coated with Co/CeO_2 catalysts. Int J Hydrogen Energy 2012;37:14812–9.
[14] Guerrero-Pérez MO, Bañares MA. From conventional in situ to operando studies in Raman spectroscopy. Catal Today 2006;113:48–57.
[15] Joint committee on powder diffraction standards. 1995.
[16] Wu Z, Li M, Howe J, Meyer HM, Overbury SH. Probing defect sites on CeO_2 nanocrystals with well-defined surface planes by Raman spectroscopy and O_2 adsorption. Langmuir 2010;26:16595–606.
[17] Zdravković J, Simović B, Golubović A, Poleti D, Veljković I, Šćepanović M, et al. Comparative study of CeO_2 nanopowders obtained by the hydrothermal method from various precursors. Ceram Int 2015;41:1970–9.
[18] Lee Y, He G, Akey AJ, Si R, Flytzani-Stephanopoulos M, Herman IP. Raman analysis of mode softening in nanoparticle $CeO_{2-\delta}$ and $Au\text{-}CeO_{2-\delta}$ during CO oxidation. J Am Chem Soc 2011;133:12952–5.
[19] Martínez-Arias A, Gamarra D, Fernández-García M, Wang XQ, Hanson JC, Rodriguez JA. Comparative study on redox properties of nanosized CeO_2 and CuO/CeO_2 under CO/O_2. J Catal 2006;240:1–7.
[20] Woods MP, Gawade P, Tan B, Ozkan US. Preferential oxidation of carbon monoxide on Co/CeO_2 nanoparticles. Appl Catal B Environ 2010;97:28–35.
[21] Vuurman MA, Stufkens DJ, Oskam A, Deo G, Wachs IE. Combined raman and IR study of $MO_x\text{-}V_2O_5/Al_2O_3$ (MO_x = MoO_3, WO_3, NiO, CoO) catalysts under dehydrated conditions. J Chem Soc Faraday Trans 1996;92:3259–65.
[22] Sedmak G, Hocevar S, Levec J. Kinetics of selective CO oxidation in excess of H_2 over the nanostructured $Cu_{0.1}Ce_{0.9}O_{2-y}$ catalyst. J Catal 2003;213:135–50.